Available online at www.sciencedirect.com

SciVerse ScienceDirect

Solar Energy 86 (2012) 2975–2985

SOLAR ENERGY

www.elsevier.com/locate/solener

Performance and cost assessment of Integrated Solar Combined Cycle Systems (ISCCSs) using CO_2 as heat transfer fluid

Giorgio Cau, Daniele Cocco, Vittorio Tola *

University of Cagliari, Department of Mechanical, Chemical and Materials Engineering, Via Marengo 2, 09123 Cagliari, Italy

Received 22 December 2011; received in revised form 5 July 2012; accepted 5 July 2012
Available online 4 August 2012

Communicated by: Associate Editor Jayant K. Nayak

Abstract

In this paper, a performance and cost assessment of Integrated Solar Combined Cycle Systems (ISCCSs) based on parabolic troughs using CO_2 as heat transfer fluid is reported on. The use of CO_2 instead of the more conventional thermal oil as heat transfer fluid allows an increase in the temperature of the heat transfer fluid and thus in solar energy conversion efficiency. In particular, the ISCCS plant considered here was developed on the basis of a triple-pressure, reheated combined cycle power plant rated about 250 MW. Two different solutions for the solar steam generator are considered and compared.

The results of the performance assessment show that the solar energy conversion efficiency ranges from 23% to 25% for a CO_2 maximum temperature of 550 °C. For a CO_2 temperature of 450 °C, solar efficiency decreases by about 1.5–2.0% points. The use of a solar steam generator including only the evaporation section instead of the preheating, evaporation and superheating sections allows the achievement of slightly better conversion efficiencies. However, the adoption of this solution leads to a maximum value of the solar share of around 10% on the ISCCS power output. The solar conversion efficiencies of the ISCCS systems considered here are slightly greater than those of the more conventional Concentrating Solar Power (CSP) systems based on steam cycles (20–23%) and are very similar to the predicted conversion efficiencies of the more advanced direct steam generation solar plants (22–27%).

The results of a preliminary cost analysis show that due to the installation of the solar field, the electrical energy production cost for ISCCS power plants increases in comparison to the natural gas combined cycle (NGCC). In particular, the specific cost of electrical energy produced from solar energy is much greater (about two-fold) than that of electrical energy produced from natural gas.

Keywords: CSP systems; Parabolic trough collectors; ISCCS; CO_2

1. Introduction

Nowadays, a large number of R&D activities are carried out in the field of solar technologies for electricity generation based on both photovoltaic and Concentrating Solar Power (CSP) systems. In particular, in the field of CSP systems, parabolic trough collectors integrated with steam Rankine cycles are today the most commercially proven technology (Fernandez-Garcia et al., 2010). In CSP plants, solar energy produces a high temperature heat transfer fluid used for feeding a Heat Recovery Steam Generator. To increase plant availability, an energy storage system is usually installed. In the last few years, in addition to steam power plants, several alternative options have been proposed, mainly based on gas turbines and combined cycle power plants. In fact, solar energy can be used to heat the compressed air in simple cycle gas turbines (Buck et al., 2002; Fisher et al., 2004; Garcia et al., 2008; Sinasi et al., 2005) or in externally fired humidified air turbine systems (Zhao et al., 2003). Nevertheless, solar energy can also be used in more complex systems, such as steam reforming processes integrated with fuel cells or gas turbines (Tamme et al., 2001; Jin et al., 2003) or combined cycle power

* Corresponding author. Tel.: +39 070 6755709.
E-mail address: tola@dimeca.unica.it (V. Tola).

0038-092X/$ - see front matter © 2012 Elsevier Ltd. All rights reserved.
http://dx.doi.org/10.1016/j.solener.2012.07.004

plants, to produce additional steam for the bottoming Rankine cycle (Behar et al., 2011; Dersch et al., 2002, 2004; Donatini et al., 2007; Horn et al., 2004; Hosseini et al., 2005; Kane et al., 2000; Montes et al., 2011; Nezammahalleh et al., 2010). In particular, in the field of large CSP plants, Integrated Solar Combined Cycle Systems (ISCCSs) are one of the most interesting options as they allow the achievement of a significant improvement in the conversion efficiency of solar energy and reduce the importance of energy storage systems. Moreover, ISCCS plants reduce solar energy production costs since the additional cost of the combined cycle steam section is lower than the overall cost of a dedicated steam power plant (Horn et al., 2004; Dersch et al., 2004; Hosseini et al., 2005).

Worldwide, current CSP generating capacity is around 1300 MW, mainly located in the United States of America and Spain; also considering CSP systems under construction or under development, overall generating capacity is more than several GW. In the US, nine Solar Electric Generating Stations (SEGSs) have been in operation since the 1980s and 1990s, in California's Mojave Desert, with an overall generating capacity of more than 350 MW, and another plant is the Nevada Solar One with a net power output of 64 MW. Spain is the world's country with the higher CSP installed capacity, thanks to fourteen 50 MW plants in operation and nine plants under construction (SolarPACES, 2012).

Regarding ISCCS, nowadays several plants are operating in Italy, Iran and North African Countries. In Italy the Archimede Project was inaugurated in July 2010 in Priolo Gargallo (Sicily), leading to a 5 MW CSP plant integrated in a combined cycle of about 750 MW. Other ISCCS power plants with a larger solar section are currently operating in Iran (467 MW, with 17 MW from solar energy), in Morocco (470 MW, with 20 MW from solar energy), in Egypt (140 MW, with 20 MW from solar energy) and in Algeria (150 MW, with 20 MW from solar energy) (SolarPACES, 2012).

As is known, for all CSP solutions solar energy conversion efficiency increases with the maximum temperature of the heat transfer fluid (HTF). Almost all parabolic trough systems in operation or under construction use thermal oil as the HTF, which presents the important drawback of a low maximum operating temperature (about 400 °C). In this framework, the Italian Archimede project has proposed the use of molten salts (60% $NaNO_3$ and 40% KNO_3) as the HTF, making it possible to reach a maximum operating temperature of about 550 °C (Giostri et al., 2012). However, the main drawback of molten salts is their high solidification temperature (about 290 °C). To replace thermal oil and maintain high HTF temperatures, one possible choice is the direct production of steam in the solar collector, as in the most recent direct steam generation (DSG) solar plants (Birnbaum et al., 2011; Montes et al., 2009, 2011; Nezammahalleh et al., 2010; Zarza et al., 2006). Another possible option is the use of gaseous fluids as the HTF. In particular, the Italian ESTATE research Project, promoted by CRS4, Sardegna Ricerche, RTM SpA, Sapio Srl and the University of Cagliari, aimed at demonstrating the use of carbon dioxide at 550 °C in parabolic trough collectors. The overall cost of the research project is estimated at 11.4 million euros, and it has been co-funded by the Italian Ministry for Universities and Scientific Research (Baistrocchi et al., 2010; Cascetta et al., 2009; Cau et al., 2010).

This paper aims to evaluate the capabilities of integrated solar combined cycle power plants to efficiently convert the high temperature thermal energy produced by parabolic solar troughs using CO_2 as the heat transfer fluid. In particular, the study proposes to evaluate the expected performance of ISCCS power plants in function of solar radiation and for different operating conditions. Moreover, a preliminary assessment of the energy production cost has also been carried out.

2. ISCCS configuration

Fig. 1 shows a simplified scheme of the Integrated Solar Combined Cycle Systems analyzed in this paper. The ISCCS includes three main sections: the solar field (SF), the solar steam generator (SSG) and the combined cycle (CC) power plant.

The solar field is based on parabolic trough collectors connected in series to achieve the required CO_2 exit temperature and in parallel to achieve the required CO_2 mass flow. Also installed in the solar field is a CO_2 compressor for circulating the heat transfer fluid from the SF to the SSG.

In the solar steam generator the CO_2 is used to produce the steam for the combined cycle power plant. In this study, two different SSG configurations are considered and compared. In the first configuration (SSG-1), the solar steam generator includes the high-pressure preheating, vaporizing and superheating sections, whereas in the second configuration (SSG-2), it includes only the high and intermediate pressure vaporizing sections. In the latter case, water preheating and steam superheating are obviously carried out in the conventional Heat Recovery Steam Generator (HRSG). Moreover, the maximum steam mass flow produced by the SSG-2 section is closely related to the maximum thermal power available in the HRSG for water pre-heating and steam superheating. On the contrary, the influence of the HRSG thermal load on steam mass flow produced by the SSG-1 section is of minor importance, as it is simply related to the increase of the mass flow inside the HRSG steam reheating section.

The combined cycle power plant includes the gas turbine, the HRSG and the steam power plant. The gas turbine and the post-combustor of the HRSG (the latter can be used to increase the combined cycle power output during nights and other periods of low solar radiation) are fueled by natural gas. The steam cycle power section is based on a triple pressure level HRSG with steam reheating. The bottom part of Fig. 1 shows the integration between the SSG section and the HRSG for the two

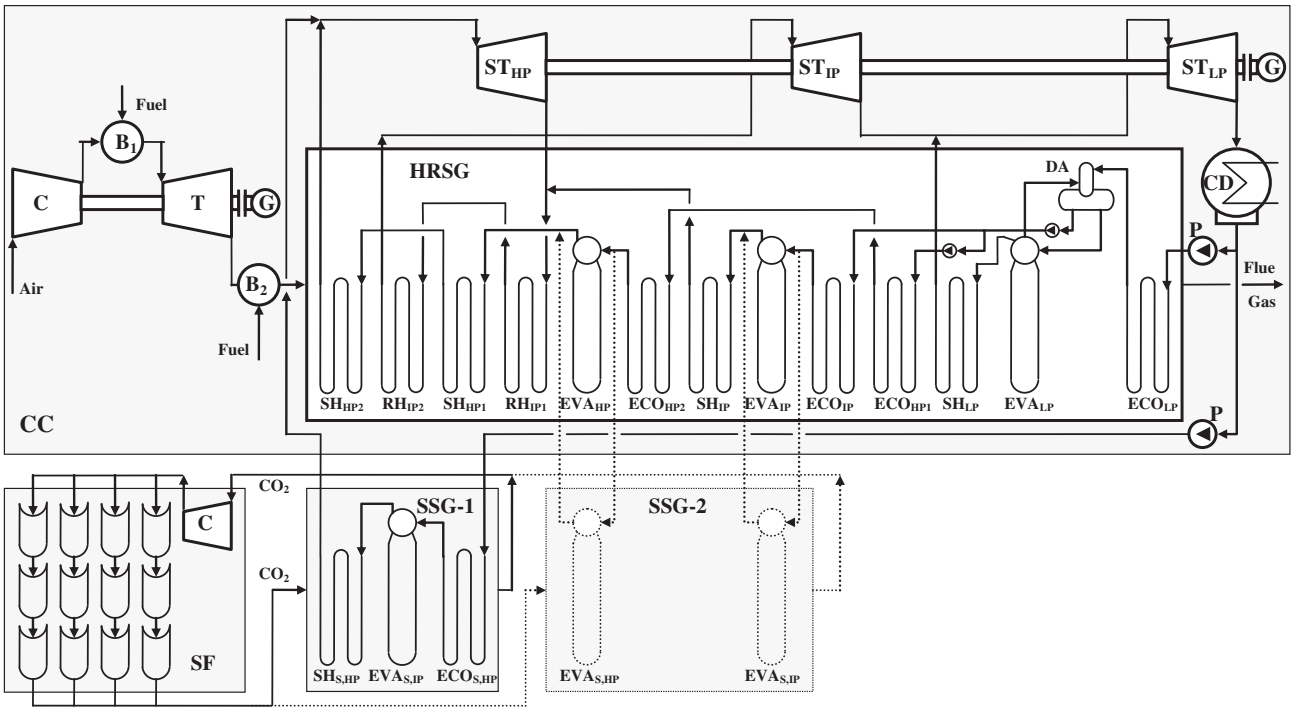

Fig. 1. Simplified scheme of the ISCCS power plant.

options considered. In the SSG-1 solution the water for the economizer is directly pumped from the condenser, while the steam is mixed with the high-pressure superheated steam produced by the HRSG. On the contrary, in the SSG-2 solution the high temperature CO_2 feeds only the high-and intermediate-pressure solar evaporators which operate in parallel with the corresponding HRSG evaporators. Water pre-heating and steam super-heating are still carried out by the HRSG of the combined cycle.

3. Solar field modeling and performance

The performance of the ISCCS plant previously described was evaluated by means of the GateCycle™ simulation software, version 5.40 (GE Enter Software, 2001). As the GateCycle™ model library does not include a solar collector, a dedicated parabolic trough simulation model was developed. The model simulates the parabolic trough performance as a function of solar radiation, technical specifications of the solar trough and composition and thermodynamic properties (pressure and temperature) of the heat transfer fluid. Thermodynamic properties of HTF were calculated through correlations from Perry and Green (1999). In particular, for given values of the mentioned inputs, the model allows evaluation of the mass flow and HTF thermal power, as well as thermal efficiency and pressure drop of the solar collector.

The simulation model was developed starting from the one-dimensional, steady-state NREL model (Forristall, 2003). In particular, it is based on the following energy balance of the solar collector:

$$\dot{Q}_{SOL} = \dot{Q}_{FLD} + \dot{Q}_{LOSS} \tag{1}$$

where $\dot{Q}_{SOL}$ denotes the solar power input (that is, the direct solar radiation available in the aperture area of the parabolic trough collector), $\dot{Q}_{FLD}$ is the solar power transferred to the heat transfer fluid, and $\dot{Q}_{LOSS}$ are the collector power losses (optical, conductive, convective and radiation). For a given collector, the simulation model allows evaluation of the temperature profile along the solar collector and the collector thermal efficiency as a function of the direct solar radiation, the mass flow and the temperature of the heat transfer fluid. In particular, according to Eq. (1), the collector thermal efficiency, and then the solar field thermal efficiency η_{SF} is represented by the ratio between $\dot{Q}_{FLD}$ and $\dot{Q}_{SOL}$:

$$\eta_{SF} = \frac{\dot{Q}_{FLD}}{\dot{Q}_{SOL}}. \tag{2}$$

In this paper the model was applied to solar parabolic troughs characterized by a length of 100 m, a collector aperture area of 576 m^2, an optical efficiency equal to 80% and a CO_2 pressure equal to 15 bar. A more detailed description of the collector simulation model can be found in Cascetta et al. (2009).

As mentioned, the main aim of the ESTATE-LAB project is to demonstrate the capabilities of parabolic solar troughs to produce high temperature gaseous fluids for feeding a solar steam generator. Previous studies show that CO_2 assures better performance in comparison to other gaseous fluids (Cascetta et al., 2009). Fig. 2 shows collector thermal efficiency as a function of the direct solar radiation incident on the collector aperture area for given values of

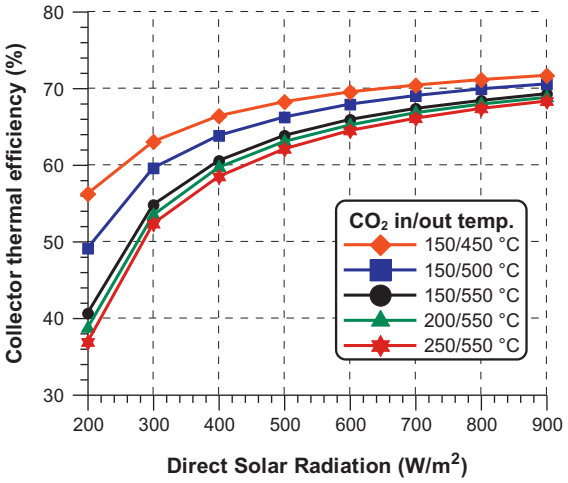

Fig. 2. Collector thermal efficiency in function of CO_2 temperatures and direct solar radiation.

both inlet (150 °C, 200 °C and 250 °C) and outlet (450 °C, 500 °C and 550 °C) CO_2 temperatures. The collector thermal efficiency increases with high values of solar radiation and with low values of the CO_2 mean temperature (maximum efficiency is reached for 150 °C at the inlet and 450 °C at the outlet). In fact, high solar radiation and low mean temperatures reduce the influence of convective and radiation energy losses. Overall, the achievement of a collector thermal efficiency higher than 70% requires a solar radiation above 800 W/m^2.

Fig. 3 shows the CO_2 mass flow and the CO_2 thermal output per unit collector aperture area as a function of the direct solar radiation and for different values of the CO_2 inlet and outlet temperatures. Both CO_2 mass flow and CO_2 thermal output increase with solar radiation due to the increase in the available solar energy and better collector thermal efficiency. Moreover, the CO_2 mass flow and the CO_2 thermal output per unit area increase with decreasing values of the CO_2 outlet temperature and with increasing values of the CO_2 inlet temperature. However, the thermal power per unit area is less influenced by the CO_2 mean temperature than the CO_2 mass flow.

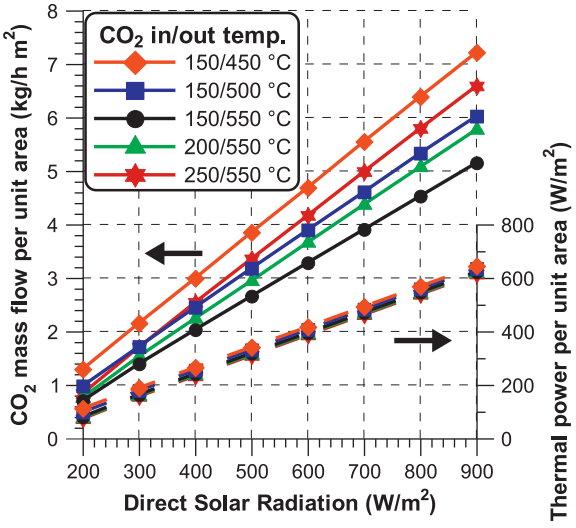

Fig. 3. CO_2 mass flow and useful thermal power in function of CO_2 temperatures and direct solar radiation.

4. Power section modeling and performance

The performance of the ISCCS power section (that is, SSG + CC) was calculated by means of the GateCycle™ simulation software starting from a combined cycle power plant based on a GEMS531(FA) gas turbine integrated with a triple pressure level HRSG. The combined cycle is rated at 252.6 MW, at ISO conditions, with a design efficiency of 54.2%. Fig. 4 shows HRSG energy balance characteristic curves for the combined cycle. The performance of the ISCCS power section was initially evaluated in function of the available CO_2 thermal power, regardless of the operating conditions of the solar field (collector thermal efficiency, solar radiation and then solar field area). The performance assessment was carried out with reference to the two SSG solutions shown in Fig. 1 and for three different values of the SSG inlet temperature (450, 500 and 550 °C). Table 1 shows the main operating parameters assumed here for the performance assessment of the power section.

Integration of the combined cycle power plant with a solar steam generator leads to an increase in steam production and thus in steam section power output. Fig. 5 shows steam mass flows produced by the SSG and steam mass flows evolving in the HP steam turbines for both SSG-1 and SSG-2 options. Fig. 5 also shows the HP steam produced by the HRSG (only for the SSG-1 option) and the steam mass flows entering the IP steam turbine (only for the SSG-2 option). All the mass flows refer to design conditions of the power section and are reported as a function of CO_2 thermal input and CO_2 temperature.

For the combined cycle power plant considered in this study, the reference HP steam mass flow (that is, without any additional steam from SSG) is around 48 kg/s. In the case of the ISCCS plant, the steam produced by the SSG

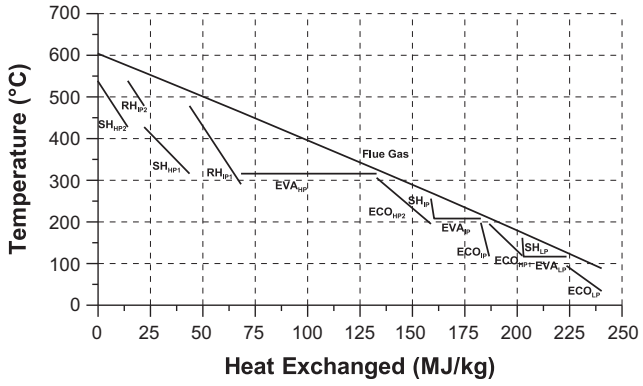

Fig. 4. HRSG energy balance characteristic curve for the reference combined cycle.

Table 1
Main operating parameters for the performance assessment of the ISCCS power section.

Gas turbine	
Gas turbine power output	165.8 MW
Gas turbine net efficiency	35.6%
Gas turbine pressure ratio	15.2
Exhaust mass flow	408.9 kg/s
Exhaust temperature	603.3 °C
Steam power plant	
ST_{HP} inlet pressure/temperature	101.3 bar/538 °C
ST_{HP} inlet mass flow	48.0 kg/s
ST_{IP} inlet pressure/temperature	16.5 bar/538 °C
ST_{IP} inlet mass flow	59.4 kg/s
ST_{LP} inlet pressure/temperature	1.65 bar/233 °C
ST_{LP} inlet mass flow	65.4 kg/s
HRSG minimum temperature difference	10 °C
Condenser pressure	0.05 bar
Steam section power output	86.8 MW
Combined cycle power output	252.6 MW
Combined cycle efficiency	54.2%
Solar steam generator	
SSG minimum temperature difference	10 °C
SSG-1 approach temperature difference	30 °C

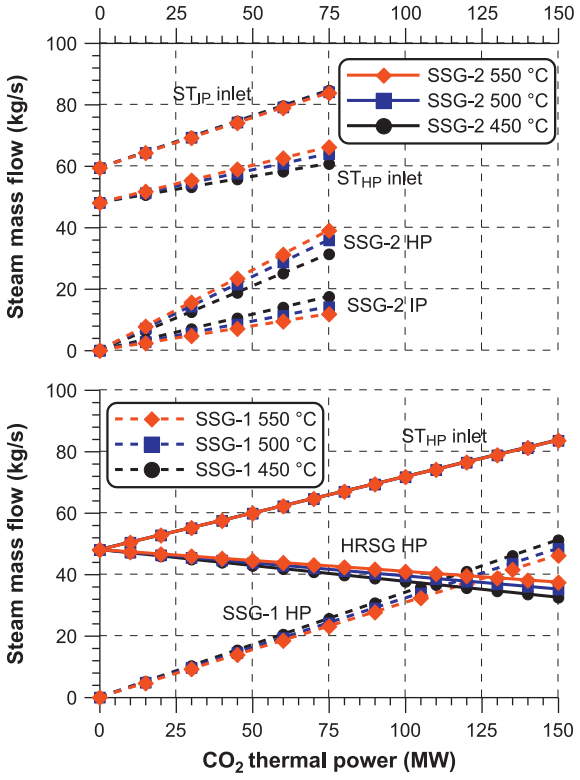

Fig. 5. Steam mass flow in function of the CO_2 thermal input and the CO_2 inlet temperature.

section increases with the available CO_2 thermal power. However, as shown by Fig. 1, the HRSG is fully integrated with the SSG-2 configuration, whereas the HRSG is only partially influenced by the presence of the SSG-1. For this reason the maximum CO_2 thermal input of the SSG-2 solution closely depends on the HRSG available heat for water preheating and steam superheating. In this analysis therefore the maximum value of the CO_2 design thermal input for the SSG-2 section has been restricted to 75 MW and that of the SSG-1 to 150 MW. Actually, too high design values of the solar thermal input can lead to a noteworthy modification of the thermal load in the different HRSG sections.

Fig. 5 shows that for the SSG-1 configuration, the HP steam produced by the solar steam generator increases with thermal power associated with CO_2, from zero up to 46–51 kg/s for a CO_2 thermal power of 150 MW (the maximum value is obtained for the lower CO_2 temperature). On the contrary, HP steam produced by the HRSG slightly decreases with CO_2 thermal power, from 48 kg/s to 32–37 kg/s for a CO_2 thermal power of 150 MW (the maximum value in this case is obtained for the higher CO_2 temperature). In fact, as mentioned before, the increase in the HP steam mass flow requires more power for the HRSG reheating section and thus decreases the heat available for the HRSG superheating section. The mass flow evolving in the HP turbine increases less than the steam produced by the SSG-1 section (from 48 kg/s to 83.5 kg/s for a CO_2 thermal power of 150 MW), due to the reduction of the steam produced by the HRSG, with no significant influence of CO_2 temperature. Similarly, the mass flow of saturated steam produced by the HP and IP evaporators of the SSG-2 section linearly increases with CO_2 thermal input, thus leading to a corresponding increase in the steam mass flow at the inlet of the HP and IP turbines. For the high pressure evaporator the maximum value of steam mass flow of 39 kg/s is obtained for a CO_2 temperature of 550 °C, whereas for the intermediate pressure evaporator the maximum value of steam mass flow of 17.5 kg/s is obtained for a CO_2 temperature of 450 °C. Despite a greater increase in the HP steam produced in the SSG-2 section in comparison to the SSG-1 configuration, the higher reduction of steam produced by the HRSG leads to a steam mass flow evolving in the HP turbine comparable to that of the SSG-1 configuration (66 kg/s for a CO_2 thermal power of 75 MW). In fact, even though for a CO_2 temperature equal to 450 °C the steam mass flow evolving in the HP turbine is equal to 60.7 kg/s, increasing the CO_2 temperature increases CO_2 mass flow up to 66.1 kg/s for a CO_2 temperature of 550 °C. Nevertheless, the decrease in saturated steam mass flow produced by the IP evaporator, thus increasing CO_2 temperature, leads to a steam mass flow evolving in the IP turbine practically not influenced by CO_2 temperature.

Fig. 6 shows the net power output gain P_{SOL} of the ISCCS power section as a function of the CO_2 thermal power, for both SSG-1 and SSG-2 configurations and for the three different values of the SSG inlet temperature considered. Overall, with an estimated pressure drop equal to 1 bar (solar field and solar steam generator), the CO_2 compressor requires 5–10% of the gross power output gain produced from the CO_2 thermal power. For a given CO_2 thermal power, the lowest power requirement obviously

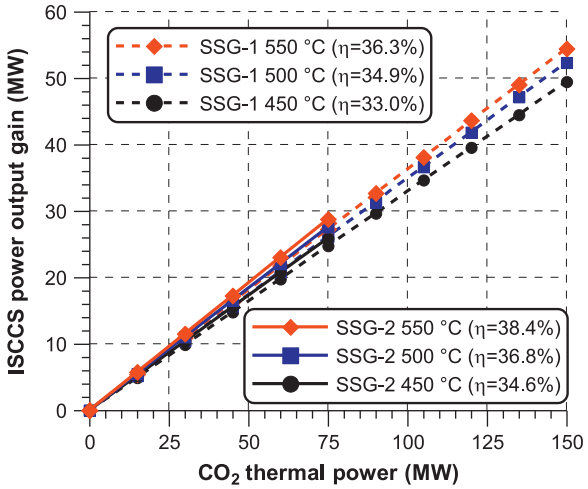

Fig. 6. ISCCS power output gain in function of CO_2 thermal input and CO_2 inlet temperature.

refers to the lowest values of both CO_2 mass flow and CO_2 compressor inlet temperature, that is, for the SSG-1 configuration and 550 °C. As appears in Fig. 6, the power output gain P_{SOL} is almost proportional to the CO_2 thermal power and increases with CO_2 temperature for both SSG configurations, even though the power output gain of the SSG-2 solution is greater than that of the SSG-1. For the SSG-2 option (maximum CO_2 thermal input equal to 75 MW) the power output gain is 28.8 MW at 550 °C (which is more than 11% of the reference combined cycle power output), whereas the maximum power output gain is equal to about 26 MW if CO_2 temperature decreases to 450 °C. As the ISCCS power plant based on the SSG-1 option allows a design for a higher CO_2 thermal input (150 MW), the maximum power output gain is 54.5 MW at 550 °C and 49.5 MW at 450 °C.

Fig. 6 also reports the conversion efficiency of the CO_2 thermal power η_{PS} (even at design conditions), here defined as the ratio between the power output gain P_{SOL} and the solar power transferred to the HTF $\dot{Q}_{FLD}$:

$$\eta_{PS} = \frac{P_{SOL}}{\dot{Q}_{FLD}}. \quad (3)$$

In the cases considered here, η_{PS} ranges from 33.0% to 38.4%. In particular, η_{PS} improves by adopting the SSG-2 solution (the efficiency improvement with respect to the use of the SSG-1 option ranges from 1.6 to 2.1 percentage points, as a function of CO_2 temperature) and also with higher values of the CO_2 temperature (the increase from 450 °C to 550 °C improves the efficiency by 3.3 percentage points for SSG-1 and 3.8 percentage points for SSG-2).

Due to the absence of the thermal storage section, the ISCCS power plants operate at part load behavior during nights and the periods of low solar radiation. In fact, the daily and seasonal variations of solar radiation lead to a corresponding variation in CO_2 thermal energy and therefore to the steam production in the SSG section. During part load behavior, ISCCS power output decreases with CO_2 thermal input, due to the lower steam production for both SSG options. Nevertheless, with respect to design conditions, the decrease in ISCCS power output is lower than 6–7%, even for a CO_2 thermal input equal to 30% of design conditions, due to the predominant contribution of the combined cycle to overall power output. For this reason, steam turbine efficiency can be assumed constant and thus the fossil fuel conversion efficiency of the ISCCS power plant can be assumed to be almost unchanged.

5. ISCCS power plant performance

For a given solar energy availability, depending on geographic location of the plant, an ISCCS power plant must be designed according to suitable reference conditions for both solar field and power section. As previously discussed, for a required CO_2 thermal power, the solar field aperture area depends on the direct solar radiation incident on the collector aperture area, as well as on the collector efficiency, which also depends on CO_2 inlet and outlet temperatures.

The solar field design of CSP systems was carried out with reference to the highest values of the direct normal irradiation (DNI), assumed as the average DNI value at noon on 21 June. The highest values of DNI in southern European countries range from 800 to 900 W/m^2. As previously mentioned, parabolic troughs use a single-axis tracking system to follow the sun's track from east to west, with no north–south tracking system. For this reason, the incidence angle of direct solar radiation on the aperture area is greater than 0° (especially during winter months) and the direct solar radiation available on the collector aperture area is lower than the DNI. Moreover, with solar fields composed of multiple rows of parabolic collectors, the shadow effects between the collector rows reduce available direct solar radiation, especially during sunrise and sunset. At the noon design point, with incidence angles around 12–16° and no shadow effects between rows of collectors, the direct solar radiation available on the aperture area is about 96–98% of the DNI.

With reference to design conditions, Fig. 7 shows the required solar field aperture area in function of the desired CO_2 thermal power for different DNI design conditions (800, 850 and 900 W/m^2) and for both SSG-1 and SSG-2 configurations. The solar field aperture area was evaluated by assuming a CO_2 temperature of 550 °C and a solar radiation available on the collector surface equal to 97% of DNI. The ISCCS based on the SSG-2 solution requires a slightly higher solar field area than the SSG-1 to achieve the same CO_2 thermal power, due to its higher CO_2 exit temperature (224 °C instead of 182 °C of the SSG-1 configuration) and thus to its lower collector thermal efficiency. In particular, for a DNI equal to 900 W/m^2 and a maximum CO_2 temperature of 550 °C, a CO_2 thermal power of 75 MW is obtained through a solar field aperture area respectively equal to 120830 m^2 for the

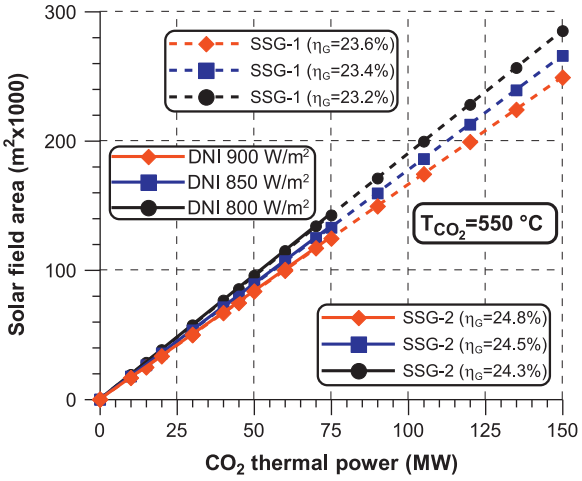

Fig. 7. Solar field aperture area in function of CO_2 thermal input.

SSG-1 configuration and to 121530 m^2 for the SSG-2 configuration. In the following analysis, performance of an ISCCS power plant based on SSG-1 and SSG-2 options was compared with reference to the same solar field based on 210 collectors, for an overall area of 120960 m^2.

Fig. 7 also reports net solar conversion efficiency η_G defined here as the ratio between the net solar power output P_{SOL} and the corresponding solar power input $\dot{Q}_{SOL}$:

$$\eta_G = \frac{P_{SOL}}{\dot{Q}_{SOL}} \tag{4}$$

Obviously, according to Eqs. (2) and (3), net solar conversion efficiency η_G is calculated by the product of solar field efficiency η_{SF} and power section efficiency η_{PS}. Similar to power section efficiency η_{PS} (see Fig. 6), net solar conversion efficiency does not in practice depend on CO_2 thermal power. Indeed, it depends only on the SSG configuration, which affects η_{PS}, and on the design DNI, which affects η_{SF}. For a ISCCS power plant with a maximum CO_2 temperature of 550 °C, net solar conversion efficiency η_G ranges from 23.2% (SSG-1 with a design point DNI of 800 W/m^2) to 24.8% (SSG-2 with a design point DNI of 900 W/m^2). ISCCS power plants based on the SSG-2 configuration assure higher net solar conversion efficiencies in comparison to SSG-1, despite their lower solar field efficiency η_{SF}, thanks to the higher power section efficiency η_{PS}. Due to the lower temperature of superheated steam produced in the SSG, a lower CO_2 temperature leads to lower solar efficiencies. For example, by assuming a CO_2 temperature of 450 °C, η_G decreases by about 1.5–1.7 percentage points (it ranges from 21.7% for the ISCCS plant based on the SSG-1 configuration with a design point DNI of 800 W/m^2 to 23.1% for the ISCCS plant based on the SSG-2 with a design point DNI of 900 W/m^2). Moreover, it should be observed that for both SSG solutions considered, ISCCS efficiency values are slightly greater than the corresponding efficiencies of conventional CSP systems based on parabolic troughs integrated with steam power plants (the net efficiency of these systems ranges from 20% to 23%) (Giostri et al., 2012) and are very similar to the predicted conversion efficiencies of the direct steam generation solar plants (22–27%) (Giostri et al., 2012; Zarza et al., 2006).

Table 2 summarizes the main process data and main performance for the reference combined cycle with no CO_2 thermal power integration and for the two ISCCS configurations (SSG-1 and SSG-2).

The annual energy production of an ISSCS power plant depends closely on direct normal radiation available for the design site. In the countries of south Europe (Spain, Italy, Greece), the annual DNI availability ranges from 1700 to 2200 kWh/m^2. Annual DNI values of more than 2500–2800 kWh/m^2 can be found in southern states of the United States (California, Arizona, Nevada, etc.) or in other countries suitable for CSP plants (Mexico, Jordan, Algeria, Morocco, etc.). In this paper, the annual performance of ISCCS power plants are evaluated with reference to the 8760 hourly values of DNI measured in Cagliari, Sardinia (Italy), in 2005.

During periods of part load behavior (that is, for a DNI lower than the reference value of 900 W/m^2), the conversion efficiency of the power section is only slightly reduced with respect to the design value. On the contrary, solar field efficiency is largely influenced by DNI, as shown in Fig. 2. In particular, solar field efficiency decreases for solar radiation values lower than the reference DNI, even if the decrease in the CO_2 temperature at the collector inlet slightly reduces the penalty on solar field efficiency due to the lower DNI (in particular, temperature decreases from 182 °C down to 150 °C for a DNI equal to 200 W/m^2 with a SSG-1 configuration and from 224 °C down to 200 °C for a SSG-2 configuration). For the reference DNI (900 W/m^2), the solar power contribution is 25.5 MW for the SSG-1 configuration and 26.8 MW for the SSG-2 configuration. In practice, the solar field guarantees a power gain respectively equal to 10.1% and 10.6% in comparison to the reference combined cycle power (252.6 MW). For both SSG solutions, the solar contribution to annual energy production is lower than that of net power output. In fact, owing to the absence of thermal storage, the annual operating hours of the solar section depend on annual DNI availability, which also varies on a yearly and daily basis. The maximum solar contribution is obviously obtained in summer, but it is zero at night and during cloudy days (in fact, in this study, the minimum DNI that assures solar field operation has been assumed equal to 200 W/m^2).

Fig. 8 shows the monthly solar contribution to the yearly net energy production of the ISCCS power plant based on the two SSG options. In particular, Fig. 8 shows the ratio between the electrical energy produced from solar radiation and the electrical energy produced by the combined cycle from natural gas at reference conditions (that is with no solar contribution). The energy contribution from the solar field is calculated as the difference between energy from ISCCS and energy from the reference NGCC. On the right of Fig. 8, the yearly average solar contribution

Table 2
Main process data and performance of ISCCS and NGCC power plants.

		NGCC	ISCCS–SSG-1	ISCCS–SSG-2
Nominal power	MW	252.6	278.1	279.4
Gas turbine power output	MW	165.8	165.8	165.8
Steam section power output	MW	86.8	112.3	113.6
Solar power gain	MW	–	25.5	26.8
ST_{HP} inlet mass flow	kg/s	48.0	65.8	65.8
ST_{IP} inlet mass flow	kg/s	59.4	78.4	83.4
ST_{LP} inlet mass flow	kg/s	65.4	85.6	83.7
SSG HP steam mass flow	kg/s	–	23.1	38.8
SSG IP steam mass flow	kg/s	–	–	11.8
Solar field aperture area	m^2	–	120960	120960
CO_2 thermal power	MW	–	75.08	74.65
Design point DNI	W/m^2	–	900	900
Maximum CO_2 temperature	°C	–	550.0	550.0
Minimum CO_2 temperature	°C	–	182.0	224.0
CO_2 mass flow	kg/s	–	188.5	224.0
Solar field thermal efficiency	%	–	65.0	64.6
CO_2 thermal power conv. efficiency	%	–	36.3	38.4
Net solar conversion efficiency	%	–	23.6	24.8

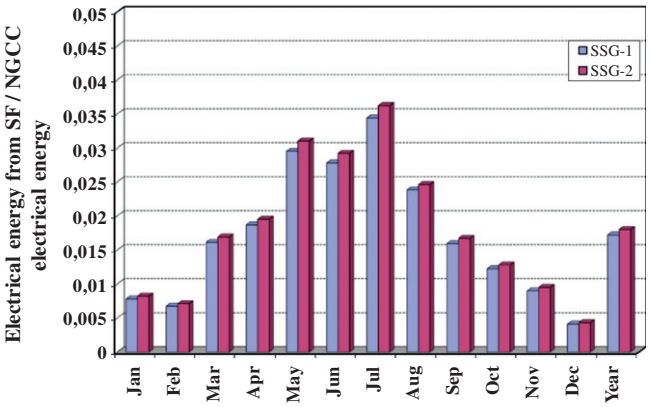

Fig. 8. Monthly ratio between energy gain due to the solar field and energy from combined cycle at reference conditions.

is also shown. During winter (from November to February) the contribution of solar radiation to ISCCS net energy production is lower than 1%, whereas during summer the solar contribution exceeds 2–3%, with maximum values of 3.4% (SSG-1) and 3.6% (SSG-2) calculated for July. The SSG-2 configuration achieves a higher solar contribution in comparison to the SSG-1 configuration due to the higher net solar conversion efficiency η_G. Globally, the annual energy gain is 1.72% (SSG-1) and 1.80% (SSG-2).

With reference to data measured during 2005 in Cagliari, a DNI annual availability of 1530 kWh/m^2 is calculated. However, owing to the minimum useful DNI value assumed here (200 W/m^2), the DNI annual availability for the ISCCS power plant decreases to 1425 kWh/m^2. The annual net electrical energy production from solar in the ISCCS plant is equal to 315 kWh/m^2 for the SSG-1 configuration and to 328 kWh/m^2 for the SSG-2 one and the net solar conversion efficiency η_G is 22.1% and 23.0%, respectively. Therefore, for the present ISCCS power plant, based on a solar field aperture area of 120960 m^2, the net electrical energy production from solar is 38.3 GWh/yr (SSG-1) and 39.9 GWh/yr (SSG-2), with a design solar power output of 25.5 MW (SSG-1) and 26.8 MW (SSG-2). Overall, the integration between a combined cycle power plant fueled with natural gas and a solar field produces a fossil fuel saving of about 1.7–1.8% on a yearly basis.

Fig. 8 is obtained starting from DNI experimental data measured over a single year (2005). For this reason, solar energy production shows an irregular behavior: for example, January and May show a great solar contribution to global energy production in comparison to February and June. For comparative purposes, the analysis was repeated referring to the monthly average values for solar radiation provided by UNI 10349 for the city of Cagliari (UNI 10349, 1994). The UNI 10349 reports the average daily solar radiation of the month, based on measurements of many years. Starting from UNI 10349 data, by means of suitable correlation, the hourly DNI average values were calculated. The highest DNI values are obviously calculated in summer (the maximum value is 730 W/m^2 at noon in July) and the lowest values in winter (for example in December all DNI hourly values are lower than 200 W/m^2).

Fig. 9 compares ISCCS performance calculated with reference to DNI values measured at Cagliari during 2005 and to DNI average values calculated through UNI 10349. As expected, energy production from the solar field calculated referring to UNI data shows a more regular trend in comparison to that calculated from 2005 data. In particular, the solar contribution calculated from UNI data is lower in the first part of the year and greater in the latter (in December global energy from the solar field is zero, as the DNI average value is always below 200 W/m^2). Nevertheless, both procedures calculate almost the same yearly mean value for the energy ratio, varying from 1.72% (2005 data) to 1.74% (UNI data). The solar contribution

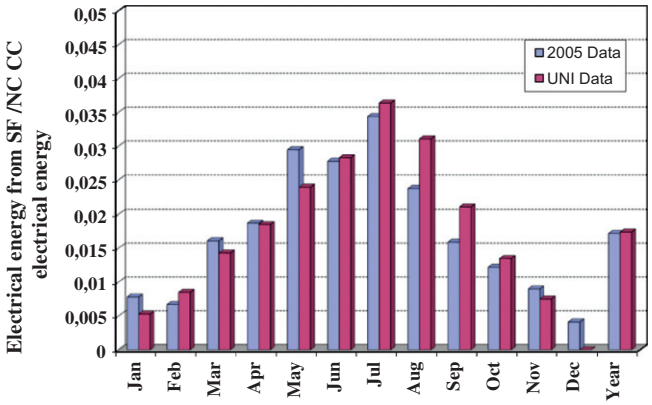

Fig. 9. Monthly ratio between energy gain due to the solar field and energy from the combined cycle at reference conditions.

in Fig. 9 refers to the energy production calculated for the SSG-1 configuration, but similar results have been obtained for the SSG-2 configuration.

6. Economic analysis

Finally, a preliminary economic analysis was carried out to compare the energy production cost of the two ISCCS power plants considered in this paper and a conventional combined cycle power plant fueled by natural gas (NGCC). In particular, the economic analysis makes it possible to calculate the Levelised Cost of Energy (LCOE) and, for the ISCCS power plant, also the solar marginal Levelised Cost of solar Energy ($LCOE_{s,m}$). The ISCCS and NGCC power plants are based on the same combined cycle and the main economic assumptions, referred to 2010, are reported in Table 3.

The LCOE is calculated with reference to the IEA (International Energy Agency) simplified methodology:

$$LCOE = \frac{(FCR - C_C + C_{O\&M} + C_F)}{E_A} \quad (5)$$

where C_C is the capital cost, $C_{O\&M}$ are the yearly operation and maintenance costs, C_F is the annual fuel cost and E_A is the annual energy production. The Fixed Charge Rate (FCR) is calculated with the following equation:

Table 3
Main assumptions for the economic analysis of ISCCS and NGCC power plants.

Specific investment cost of CC steam unit	€/kW	645
Specific investment cost of gas unit	€/kW	220
Specific investment cost of solar field	€/m^2	220
O&M cost factor of CC steam unit	%C_C	2
O&M cost factor of gas unit	%C_C	5
O&M cost factor of solar field	%C_C	1.5
Specific land cost	€/m^2	2
Natural gas price	€/t	450
Real debt interest	%	8
Annual insurance rate	%	1
Operating lifetime	Years	25

$$FCR = \frac{[(1+i)^N - i]}{[(1+i)^N - 1]} + I_{INS} \quad (6)$$

where i is the real debt interest, N is the operating lifetime and I_{INS} is the annual insurance rate. For ISCCS power plants, the LCOE calculated according to Eq. (5) refers to the energy production cost of both fossil and solar energy. As the NGCC and ISCCS configurations are based on the same combined cycle, the solar energy production cost has been evaluated by means of the solar marginal Levelised Cost of Energy, $LCOE_{s,m}$. This parameter is defined as the ratio between the increase of the annual cost of ISCCS plants with respect to NGCC plants (due to introduction of the solar field and to the higher size of the steam power section) and the corresponding increase in annual energy production due to the solar energy contribution. Table 4 shows the main results of the economic analysis.

Both ISCCS power plants are characterized by a greater nominal power in comparison to NGCC, due to the presence of the solar field which requires the steam turbine to be slightly oversized. In particular, NGCC shows a nominal power of 252.6 MW, whereas for the two ISCCS configurations the nominal power increases up to 278.1 MW (SSG-1) and to 279.4 MW (SSG-2). As previously mentioned, the power output gain of ISCCS configurations is closely related to the larger size of the steam section. For this reason, the specific investment cost (€/kW) of the combined cycle section increases and shows its maximum value for the SSG-2 configuration (392.8 €/kW). The cost of the solar field is equal to 27.12 M€ for both SSG options, as it depends on collector aperture area. Overall, the capital cost required by ISCCS power plants is about 50% higher than that of the NGCC plant, even though it leads to a power output increase of about 10% and an energy production increase of only about 2%.

Annual fuel consumption is constant for the three different solutions, as it depends only on the gas turbine rating; consequently also the annual fuel cost shows no variations (137.8 M€/y). Annual O&M costs are on the order of 3–4 M€ and increase with the size of the plant. The annual energy production of NGCC is 2212.8 GWh, and that of ISCCS plants increases by 38.1 GWh (SSG-1) and 39.7 GWh (SSG-2) due to the presence of the solar field. Overall, LCOE values (c€/kWh) are very similar, due to the small contribution of solar energy (only 1.5–2.0% of the annual energy production). LCOE results 6.79 c€/kWh for the NGCC and increases up to 6.91 c€/kWh for both ISSCS. The solar marginal Levelised Cost of Energy is significantly higher (about two-fold) than LCOE of combined cycles fueled by natural gas (13.5–14.0 c€/kWh vs. 6.8 c€/kWh). Moreover, $LCOE_{s,m}$ is higher for the SSG-1 configuration in comparison to the SSG-2 configuration, due to the higher efficiency of the SSG-2 configuration. The latter results agree with those of other economic studies on ISCCS power plants. For example, Horn et al (2004) have shown that ISCCS based on conventional HTF (thermal oil) are characterized by a $LCOE_{s,m}$ about 3–4 times

Table 4
Main results of the economic analysis of ISCCS and NGCC power plants.

		NGCC	ISCCS–SSG-1	ISCCS–SSG-2
Nominal power	MW	252.6	278.1	279.4
Specific investment cost of CC	€/kW	366.0	391.7	392.8
Cost of solar field	M€	–	27.1	27.1
Total investment cost	M€	92.69	136.25	137.10
Annual investment cost	M€/y	9.61	14.13	14.21
Annual fuel cost	M€/y	137.79	137.79	137.79
Annual O&M cost	M€/y	2.94	3.67	3.69
Total annual cost	M€/y	150.34	155.59	155.69
Annual electricity production	GWh/y	2212.8	2250.9	2252.5
LCOE	c€/kWh	6.79	6.91	6.91
$LCOE_{s,m}$	c€/kWh	–	13.77	13.48

higher than the LCOE of a combined cycle fueled by natural gas. Montes et al. (2011) have recently shown that more innovative ISCCS based on direct steam generation give an $LCOE_{s,m}$ about twice that of NGCC–LCOE in the case of installation in Southern Europe, whereas the levelised costs of energy of ISCCS and NGCC are comparable for typical solar irradiation of Southern US. It is important to point out that calculated Levelised Cost of Energy strictly depends on both specific plant design and cost assumptions of the economic analysis. In this framework a sensitivity analysis was carried out to evaluate the influence of both fuel price and solar field specific cost on the solar energy marginal cost. In fact, with the development of solar technologies a great reduction in solar field costs is expected, with a corresponding reduction of $LCOE_{s,m}$. At the same time, the natural gas cost is expected to increase in the future, thus increasing NGCC–LCOE and reducing the gap with $LCOE_{s,m}$.

Fig. 10 shows LCOE of NGCC and $LCOE_{s,m}$ of ISCCS (for both SSG-1 and SSG-2 configurations) as a function of solar field cost, for a natural gas reference cost of 450 €/t. The SSG-2 configuration provides the lower $LCOE_{s,m}$ and the breakthrough point between LCOE and $LCOE_{s,m}$ is reached for a solar field cost of 35 €/m^2. Fig. 11 shows the same economic parameters as a function of natural gas price for a solar field reference cost of 220 €/m^2. The breakthrough point between LCOE and $LCOE_{s,m}$ is reached for a natural gas price equal to 935 €/t (SSG-2) and 955 €/t (SSG-1) respectively.

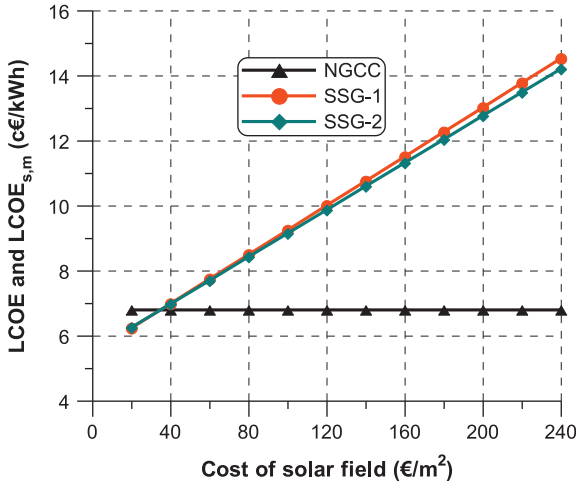

Fig. 10. Levelised Cost of Energy of NGCC and solar marginal Levelised Cost of Energy of ISCCS as a function of cost of the solar field.

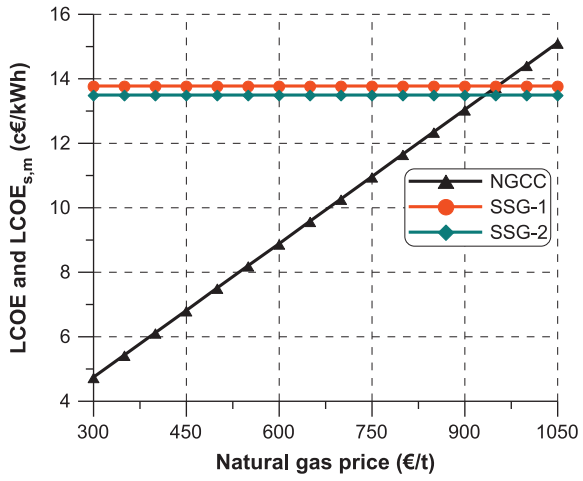

Fig. 11. Levelised Cost of Energy of NGCC and solar marginal Levelised Cost of Energy of ISCCS as a function of natural gas price.

7. Conclusions

The performance assessment carried out in this paper demonstrates that Integrated Solar Combined Cycle Systems (ISCCSs) may be an interesting option for Concentrating Solar Power (CSP) power plants based on parabolic solar troughs, especially when CO_2 is used as the heat transfer fluid. In fact, the results of the performance assessment show that net solar energy conversion efficiency ranges from 23% to 25% for a CO_2 maximum temperature of 550 °C. ISCCS efficiency is slightly higher than that of the conventional CSP systems based on steam cycles (20–23%) and is very similar to the predicted conversion efficiencies of the more advanced direct steam generation solar power plants (22–27%). In the study also a comparison between a solar steam generator equipped with

preheating, evaporating and superheating sections (SSG-1) and one with only the evaporating section (SSG-2) was also performed. Overall, the ISCCS plant based on the SSG-1 solution assures a higher solar power share, whereas an ISCCS plant based on the SSG-2 configuration provides slightly better conversion efficiencies.

In a ISCCS power plant the solar contribution to energy production is obviously lower than the solar contribution to the nominal power output. In fact, due to the absence of the thermal storage section, the ISCCS power plants operate at part load behavior during nights and during periods of low solar radiation. Energy production increases by about 1.5–2.0% on a yearly basis with the introduction of the solar section, with a corresponding fossil fuel saving.

The integration of the combined cycle with solar energy, due to higher costs associated with the solar field section, increases the Levelised Cost of Energy (LCOE) from 6.79 c€/kWh (NGCC) to 6.91 c€/kWh (ISCCS). A solar marginal LCOE equal to 13.77 c€/kWh (ISCCS with the SSG-1 configuration) and 13.48 c€/kWh (ISCCS with the SSG-2 configuration) was calculated. It is expected that a widespread diffusion of solar technologies will lead to a sensible reduction of solar field costs which, associated with an expected increase in fossil fuel prices, will make ISCCS more competitive in the near future. In particular, solar marginal LCOE will equalize NGCC–LCOE for a natural gas price of about 950 €/t or a solar field cost of 35 €/m^2.

References

Baistrocchi, M., Bartolini, G., Camerada, M., Castelli, P., Cau, G., Cocco, D., D'Aguanno, B., Delussu, G., Grimolizzi, L., Mura, F., Palomba, C., Pisano, A., Puddu, P., Salimbeni, D., Usai, E., Varone, A., 2010. Parabolic trough demonstrator for high temperature solar energy in Sardinia using gas as heat transfer fluid. In: Solar Paces 2010, Perpignan, France.

Behar, O., Kellaf, A., Mohamedi, K., Belhamel, M., 2011. Instantaneous performance of the first Integrated Solar Combined Cycle System in Algeria. Energy Procedia 6, 185–193.

Birnbaum, J., Feldhoff, J.F., Fichtner, M., Hirsch, T., Jöcker, M., Pitz-Paal, R., Zimmermann, G., 2011. Steam temperature stability in a direct steam generation solar power plant. Solar Energy 85 (4), 660–668.

Buck, R., Braeuning, T., Denk, T., Pfaender, M., Schwarzboezl, P., Tellez, F., 2002. Solar-hybrid gas turbine-based power tower systems. Journal of Solar Energy Engineering: Transactions of ASME 124.

Cascetta, M., Cau, G., Cocco, D., Puddu, P., 2009. Il Progetto ESTATE-LAB: un impianto solare termodinamico operante con fluidi termovettori gassosi ad alta temperatura. In: 64th ATI Congress, L'Aquila, Italy.

Cau, G., Cocco, D., Concas, P., Tola, V., 2010. Integration of combined cycle power plants and parabolic solar troughs using CO_2 as heat transfer fluid. In: ASME Turbo Expo 2010, GT2010-22886, Glasgow, Scotland.

Dersch, J., Geyer, M., Hermann, U., Jones, S.A., Kelly, B., Kistner, R., Ortmanns, W., Pitz-Paal, R., Price, H., 2002. Solar trough integration into combined cycle systems. In: 2002 International Solar Energy Conference, SED2002-1072, Reno, Nevada, USA.

Dersch, J., Geyer, M., Herrmann, U., Jones, S.A., Kelly, B., Kistner, R., Ortmanns, W., Pitz-Paal, R., Price, H., 2004. Trough integration into power plants – a study on the performance and economy of Integrated Solar Combined Cycle Systems. Energy 29, 947–959.

Donatini, F., Zamparelli, C., Maccari, A., Vignolini, M., 2007. High efficiency integration of thermodynamic solar plant with natural gas combined cycle. In: 2007 International Conference on Clean Electrical Power, ICCEP '07, Art. No. 4272472, pp. 770–776.

Fisher, U., Sugarmen, C., Ring, A., Sinasi, J., 2004. Gas turbine solarization – modifications for solar/fuel hybrid operation. Journal of Solar Energy Engineering 126, 872–878.

Forristall, R., 2003. Heat transfer analysis and modeling of a parabolic trough solar receiver implemented in engineering equation solver. NREL/TP-550-34169.

Fernandez-Garcia, A., Zarza, E., Valenzuela, L., Perez, M., 2010. Parabolic trough solar collectors and their applications. Renewable and Sustainable Energy Reviews 14 (2010), 1695–1721.

Garcia, P., Ferriere, A., Flamant, G., Costerg, P., Soler, R., Gagnepain, B., 2008. Solar field efficiency and electricity generation estimations for a hybrid solar gas turbine project in France. Journal of Solar Energy Engineering 130, 014502.

Giostri, A., Binotti, M., Astolfi, M., Silva, P., Macchi, E., Manzolini, G., 2012. Comparison of different solar plants based on parabolic trough technology. Solar Energy.

Horn, M., Führing, H., Rheinländer, J., 2004. Economic analysis of Integrated Solar Combined Cycle power plants. A sample case: the economic feasibility of an ISCCS power plant in Egypt. Energy 29, 935–945.

Hosseini, R., Soltani, M., Valizadeh, G., 2005. Technical and economic assessment of the integrated solar combined cycle power plants in Iran. Renewable Energy 30, 1541–1555.

Jin, H., Hong, H., Ji, J., Wang, Z., Cai, R., 2003. Solar upgrading of methanol – driven combined cycle using middle temperature solar collectors. In: International Solar Energy Conference, ISEC2003-44044, Hawaii, USA.

Kane, M., Favrat, D., Ziegler, K., Allani, Y., 2000. Thermoeconomic analysis of advanced solar–fossil combined power plants. International Journal of Applied Thermodynamics 3, 191–198.

Montes, M.J., Abánades, A., Martínez-Val, J.M., 2009. Performance of a direct steam generation solar thermal power plant for electricity production as a function of the solar multiple. Solar Energy 83, 679–689.

Montes, M.J., Rovira, A., Munoz, M., Martinez-Val, J.M., 2011. Performance analysis of an integrated solar combined cycle using direct steam generation in parabolic trough collectors. Applied Energy 88 (9), 3228–3238.

Nezammahalleh, H., Farhadi, F., Tanhaemami, M., 2010. Conceptual design and techno-economic assessment of Integrated Solar Combined Cycle System with DSG technology. Energy Procedia 6, 186–194.

Perry, R.H., Green D.W., 1999. Perry's Chemical Engineers' Handbook, Seventh ed., McGraw-Hill.

Sinasi, J., Surarmen, C., Fisher, U., 2005. Adaptation and modification of gas turbines for solar energy applications. In: ASME Turbo Expo 2005, GT2005-68122, Reno, Nevada, USA.

Tamme, R., Buck, R., Epstein, M., Fisher, U., Sugarmen, C., 2001. Solar upgrading of fuels for generation of electricity. Journal of Solar Energy Engineering 123, 160–163.

UNI 10349, 1994. Riscaldamento e raffrescamento degli edifice. Dato Climatici.

Zarza, E., Rojas, M.E., Gonzalez, L., Caballero, J.M., Rueda, F., 2006. INDITEP: the first pre-commercial DSG solar power plant. Solar Energy 80, 1270–1276.

Zhao, H., Hongguang, J., Cai, R., 2003. Solar energy utilization in externally fired humidified air turbines. In: 2003 International Solar Energy Conference, ISEC2003-44062, Hawaii, USA.

GE Enter Software, LLC., Gate Cycle 5.40, 2001. <www.gepower.com>.

SolarPACES, 2012. <http://www.solarspaces.org>.